INTERFACIAL DAMAGE AND LOAD TRANSFER MODELING IN SHORT FIBER REINFORCED COMPOSITES

K. Bonnay, N. Despringre, Y. Chemisky, F. Meraghni

Arts et Métiers ParisTech Metz, LEM3 UMR CNRS 7239, Metz, France
Email: fodil.meraghni@ensam.eu

Keywords: Interface, Decohesion, Cohesive zone, Composite, Damage

Abstract
Due to the compromise between their thermomechanical properties and low density, Short Fiber Reinforced Polyamides (SFRP) present a good alternative to metals for automotive structural components. The microstructure of such materials, combined with the matrix sensitivity to environmental conditions, has a strong impact on their overall behavior and the related damage. A new multi-scale modelling strategy is proposed, based on the experimental observations of interfacial damage evolution for PA66-GF30 composites.
Three main key-points have been integrated to this approach: an original damage evolution law at the interface, an appropriate load transfer law at the matrix-fiber interface, and a homogenization strategy founded on the generalized Mori-Tanaka scheme. The damage evolution law is driven by a local probabilistic criterion based on the interfacial stress field estimation. This type of evolution depends on the maximal local damage rate at the fiber/matrix interface, determined from a numerical evaluation at several points of the interface surrounding the inclusion. It is then coupled with a load transfer law formulated according to a modified shear lag model (SLM). The developed model is assessed with a finite element (FE) computation integrating cohesive elements at the matrix-fiber interface. The FE unit cell consists in a periodic media (hexagonal array) with periodic boundary conditions. The fiber-matrix interface integrates cohesive elements, with a cohesive law driven by a Paulino-Park-Roesler (PPR) potential-based formulation. The latter has been proven to be suitable for the 3D modeling of interface in reinforced composites. The proposed approach is able to accurately capture the non-linear behavior of short fiber reinforced polyamide composites accounting for interfacial damage.

1. Introduction

Short fiber reinforced composites (SFRC) provides high thermomechanical performances and good density ratio allowing lightweight structural parts in automotive industry. The microstructure of such materials strongly impacts their behavior and their damage evolution. Different degradation mechanisms appear at the microscopic level as the interfacial debonding, matrix microcracks and fiber breakage [1, 2]. Interfacial decohesion is considered as the predominant one playing a crucial role in the effective behavior. To predict the overall macroscopic behavior, the knowledge of the local stress state in the constituting phases is necessary through a suitable multiscale modeling. Defects evolution and voids density can be computed as functions of local stresses [3]. The evolution of the load transfer is not sufficiently considered to integrate the damage at the fiber-matrix interface.
In past decades, the interface damage of composite materials was the subject of many intentions. In reference [4], a method considering the fiber coating has been used. Some works introduced imperfect interfaces to take into account displacement and stress jump at the interface between two constituents

Excerpt from ISBN 978-3-00-053387-7

of a material [5, 6]. Others consider imperfectly bonded interfaces [7]. In [8], a new solution of the eigenstrain problem of a spherical inclusion with an imperfect interface has been determined. The shear lag method (SLM), originally proposed in [9], provides a powerfull alternative to predict stress state of a fiber inside a stiffer matrix. Recently, Jain et al. [10] have developed an equivalent debonded inclusion model for Eshelby based approaches coupled with the Cox's predictions applied for six loading cases, namley three uniaxial tensile and three shear loads.
This method, considering no slip at the interface, introduces a redistribution of strain and stress within the composite due to fiber presence. A shear stress, depending on the two phases of the composties, governs the load and the stress transfer to fibers. More details on the SLM are available in [11, 12].
The presented approach in this paper is a combination of a load transfer model based on the SLM and an interfacial damage law. This leads to the computation of the stress fields of each phases using the stress transfer ratio and the concentration tensor obtained from the adopted micromechanical homogenization scheme. The method associated to an incremental multiscale method capturing the nonlinear behavior of the interface and the composite phases.
Section 2 is dedicated to experimental observations of interfacial damage in SFRC justifying the choice of the SLM. Section 3 presents the new proposed approach. Section 4 provides a finite element (FE) model which will be used to produce a reference solution in order to validate the new approach. Section 5 focus on the results of the validation. A short conclusion will end the paper leading to some thoughts for further work.

2. Experimental observation of interfacial damage in a SFRC

Short glass fibers reinforced polyamide-66 damage mechanicms has been severaly characterised in situ under quasistatic monotonic loading. Arif et al. [13] have proposed a damage scenarios depending on the relative humidity (RH). 1) the damage starts where local stress are highest which is most of the time localised at the fiber ends (Fig. 1b). 2) interfacial decohesion propagates along the fiber interface (Fig. 1a). 3) matrix microcracks develop and propagate in various way depending on the RH. 4) accumulation of microcracks leads to failure of the material.

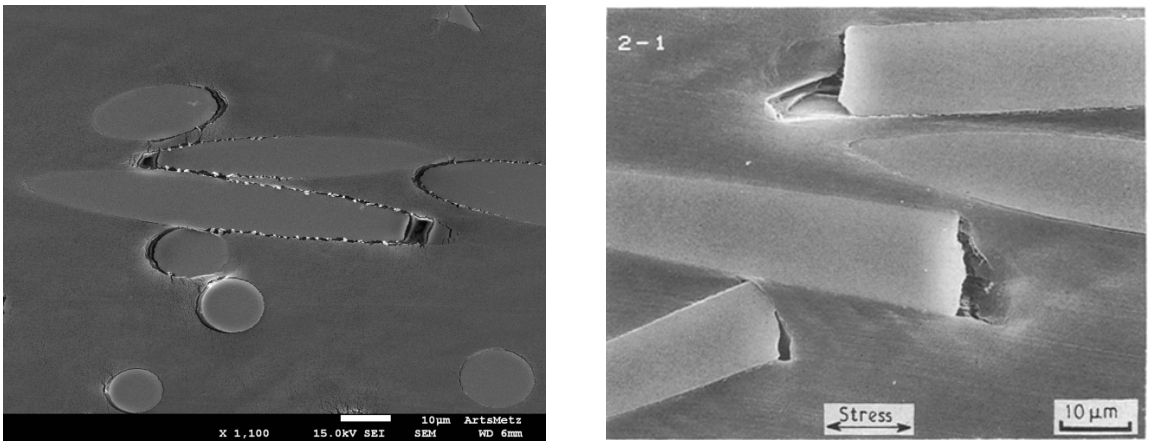

(a) (b)

Figure 1: SEM observations of the interfacial debonding of PA66GF30 obtained by (a) Arif et al. [1] which confirm those from Sato et al. [2] (b).

To be predictive, micromechanical models need to include the interfacial decohesion phenomenon. It is necessary to determin the local stress state for each phase in order to know the local state of damage. For this, the stress transfer ratio is needed to compute the stress state of fibers, and so the overall stress distribution.

Excerpt from ISBN 978-3-00-053387-7

In reference [1], the main features of defects, such as volume, orientation and shape, have been obtained for several levels of damage. They conclude that the orientation of defects follow the orientation of fibers which increases throughout the lifetime of the composite. It yields that the interfacial debonding appears as the prominent damage mechanism. While it is difficult to directly relate the quantity of defects oriented in the fiber direction to an evolution law of the interface decohesion surface, it is however demonstrated that such an evolution equation drives the overall behavior of the composite.

3. A new shear lag based method

The experimental observations help to construct an Eshelby based homogenization strategy integrating the developed interface damage evolution law coupled to an adapted load transfer model.

3.1. Damage evolution law

The damage evolution law is formulated using a quadratic rupture criterion of the local stress (Eq. 1). The shear and normal stress components are computed at each point of an ellipsoid surface. A scale factor η allows to describe the damage evolution in a family of reinforcements that share some common features, for instance orientation and aspect ratio.

$$\xi(\sigma_n, \tau) = \left(\frac{\sigma_n}{\eta\sigma_{crit}}\right)^2 + \left(\frac{\tau}{\eta\tau_{crit}}\right)^2 \leq 1 \tag{1}$$

η is introduced in the criterion as a probabilistic factor. The damage criterion (Eq. 1) can be introduced in a normalized probalistic rupture approach (Eq. 2) based on a normal law $\mathcal{N}$.

$$\tilde{P}_r(\sigma_n, \tau) = \frac{\mathcal{N}\left((C_0/C)^\alpha \xi^\gamma, m, sd\right) - \mathcal{N}\left(\kappa, m, sd\right)}{1 - \mathcal{N}\left(\kappa, m, sd\right)} \tag{2}$$

The normal law has a mean value $m = \frac{1+\kappa}{2}$ and a standard deviation $sd = sd_0\,(1-\kappa)$ where κ is the damage threshold and sd_0 is the standard deviation which allows for reaching a damage level of 99% for $\kappa = 0$, when the failure criterion is reached. γ is a shape function parameter of fibers.
In the proposed model, it is worth mentioning that the damage evolution is assumed to be correlated with the local curvature of the fibers envelope. This aspect is taken into account through the ratio of the gaussian curvature C of the considered surface point to the gaussian curvature along the central equator of the short fiber C_0. α is an exponent parameter that can adjust the damage location.

This Weibull-like statistical approach is here designed to fit in an incremental homogenization scheme. An evolution equation (Eq. 3) for the local damage of each material point at the reinforcement/matrix interface is proposed, that accounts for the actual damage d representative of the damage for the whole interface and ω which is a parameter expressing the effect of the accumulated damage on its own evolution. λ is a time normalization constant.

$$\dot{d}_{loc} = \frac{(1-d)^\omega}{\lambda} * \tilde{P}_r(\sigma_n, \tau) \tag{3}$$

The local damage criterion is computed over the entire envelope of the reinforcement using two angle : u (angle between the vector x and the projection of the normal vector in the $x0y$ plane) and v (angle between

Excerpt from ISBN 978-3-00-053387-7

the vector z and the projection of the normal vector in the $x0z$ plane). Fig. 2 shows the ellipsoidal fiber with the criterion ξ computed accordingly, and a damage map using the two integration angles u and v (both in longitudinal-transverse planes). As shown in figure 2, the computation of damage should not be restricted to the fiber ends only, even though it is commonly admitted to be the most frequent case.
The maximal local damage rate is therefore selected as the representative damage rate of the whole interface and so $\dot{d} = \max\left(\dot{d}_{loc}\right)$.

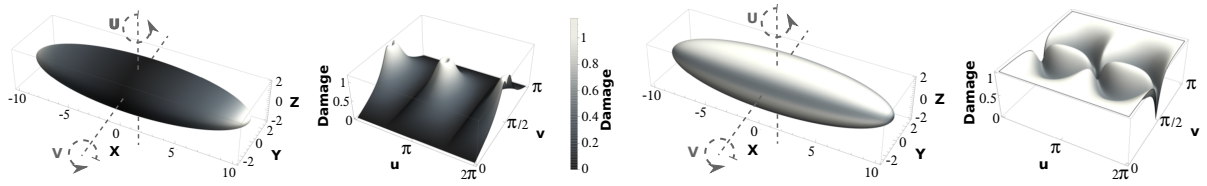

(a) Under tensile. (b) Under transverse-transverse shear.

Figure 2: Local damage criterion ξ on one reinforcement surface under tensile and under transverse-transverse shear. According to a Tresca criterion, the maximum shear stress $\tau_{crit} = \sigma_{crit}/2$, and η is equal to 1. The graph is a damage map using the two orientation angles u and v in the planes $x0y$ and $x0z$, respectively.

3.2. Load transfer model

The approach developed here is derived from a modified shear lag model (SLM) approach to define an appropriate load transfer ratio, characteristic of the stress state of a fiber. The SLM, defined by Cox [9], is originally based on the cylindrical fibers where decohesion is supposed to appear at the fibers ends.
The SLM derives a differential, defining the stress of a fiber section defined by its coordinate z, and is then integrated into Eq. 4 assuming, for the boundary conditions, that there is no stress at the fiber ends. In this equation, l is the length of the fiber, β is the shear lag parameter as defined by McCartney [14], $\langle\sigma_f\rangle$ is the average fiber stress and $\langle\sigma_{f\infty}\rangle$ is the average theoretical fiber stress if the fiber was an infinite cylinder.

$$\frac{\langle\sigma_f\rangle(z)}{\langle\sigma_{f\infty}\rangle} = 1 - \frac{\cosh(\beta z)}{\cosh(\beta\frac{l}{2})} \tag{4}$$

Eq. 4 is integrated on the whole fiber to get a load transfer ratio ψ_0 between the coating and the fiber (Eq. 5).
Since the following model is intended to be implemented into an homogenization scheme, the theoretical fiber stress $\sigma_{f\infty}$ is assumed to be determined from the homogenization method. For short fiber reinforced composites, since the aspect ratio is still rather important (at least $\approx$ 10), the reinforcement can be considered both as an ellipsoid for the homogenization method and as an infinite fiber to fulfill the requirements of the shear lag model. A similar technique has been adopted by Jain et al. [10] in their relevant work devoted to modeling partially debonded interfaces.
The global load transfer ratio (Eq. 5) is illustrated in Fig. 3. The global load transfer is represented as a function of the interfacial damage. First slightly affected with damage, the load transfer begins to drastically decrease. The load transfer eventually reaches 0% when the whole fiber interface is debonded.

$$\Psi_0 = 1 - \frac{2\tanh(\frac{l}{2}\beta)}{l\beta} \tag{5}$$

The damage parameter is then used to decrease the effective fiber length regarding load transfer. The

Excerpt from ISBN 978-3-00-053387-7

latter is in fact reduced by the damage percent. Due to the boundary conditions at the end of the fibers, the load transfer ratio is not equal to 1 when the fiber is considered to be totally bounded, in terms of its bounded length. A normalisation is thus performed to ensure that 100% load transfer to the fiber in a virgin material, leading to the final formula (Eq. 6).

$$\Psi = \left(1 - \frac{2\tanh(\frac{l(1-d)}{2}\beta)}{l(1-d)\beta}\right)/\Psi_0 \tag{6}$$

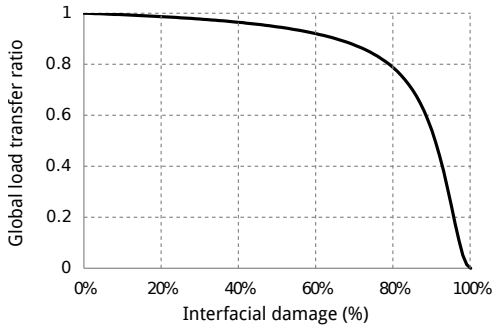

Figure 3: Shear Lag Model (SLM) based transfer load computed according to Eq. 6 for the entire fiber after normalization and as a function of interface damage.

4. FE model for validation

A 3D finite element model (Fig. 4) is developed to validate the new proposed approach. A representative volume element (RVE) composed of two fibers in a matrix has been discretized. Fibers have an ellispoidale shape. The first fiber is localized at the center of the RVE and the second one is distributed on the eigth corners of the cubic RVE as shown in Fig. 4. The geometry and the mesh are periodic which allows to apply periodic boundary conditions. Those are applied using constraint drivers [15] and the closest node from center of the RVE is totally clamped. To consider interfacial debonding between fibers and the matrix, cohesive elements are integrated in the model [16]. Those elements follow a potential-based formulation providing a flexible traction-separation law proposed by Park et al in reference [17]. C3D4 elements were adopted to model the matrix (54588 elements) and the fibers (239860 elements), and pentahedric elements were employed for the interfaces (13856 elements).

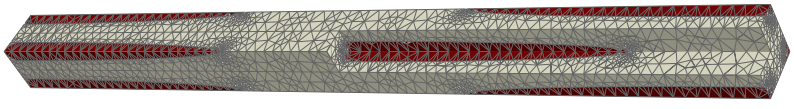

Figure 4: FE models with cohesive elements on the interface between the matrix and short fibers modeled as ellipsoidal inclusions ($AR = 22$,$V_f = 0.18$).

This RVE allows to model the PA66-GF30 composites. Parameters of the cohesive elements are chosen as follows: $\Phi_n = 1.36$ kN/m, $\Phi_t = 2.67$ kN/m, $\zeta_n = \zeta_t = 5$ and $\lambda_n = \lambda_t = 0.005$. Φ_n and Φ_t are provided by [18]. ζ_n and ζ_t are chosen to obtain a quick total failure condition when softening appears. λ_n and λ_t are chosen to obtain the lowest value of ratio of the critical crack opening width to the final crack opening width. The normal cohesive strength σ_{crit} is equal to $118MPa$. Based on the Tresca criterion, the tangential cohesive strengths τ_{crit} is equal to half of the normal cohesive strengths σ_{crit}. Elastic behaviors are considered in the matrix ($E_0 = 3.6$ GPa and $\nu_0 = 0.36$) and in the fibers ($E_1 = 72$ GPa and $\nu_1 = 0.26$). Dimensions of fibers are governed by the volume fraction ($V_f = 18\%$) and their aspect ratio ($AR = 22$).

Excerpt from ISBN 978-3-00-053387-7

5. Validation of the model

Tensile tests with various loading directions have been simulated: 0^o (in the direction the fiber), 15^o, 20^o, 45^o and 90^o.
A view of von Mises stresses resulting from the FE simulation of the PA66-GF30 in case of a loading at 0^o (in the direction of the fiber) are shown in Fig. 5. For a better observation of the debonding, the displacement scale factor is set to 10 and only half of the RVE is shown.

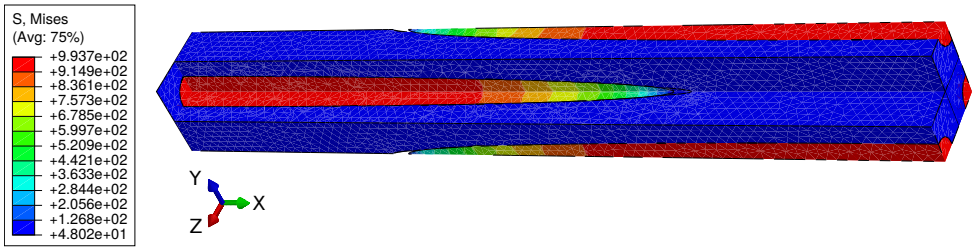

Figure 5: View of the Von Mises stresses and of the debonding on the FE models considering the PA66-GF30 at 1.5% of strain in the case of loading oriented in the direction of the fiber (0^o). Strain is zoomed X10. Only half of the RVE is represented.

As shown in Fig. 5, in this loading case, the debonding starts at the fiber ends where the stresses are maximum. It spreads then along the reinforcement. The interfacial damage reduces the stress level at the fiber extremities but the Von Mises stresses are still high at the center of the fiber. Theses observations are in agreement with the shear-lag approach.

To be able to compare the proposed model with the FE approach, a two-phase composite micromechanical simulation using the Mori-Tanaka scheme. According to the evolution of the volume fraction of the phases, an incremental version of the Mori-Tanaka scheme is adopted, in a similar way of [19, 20].
The FE strain-stress curves are used as master curves to identify the new approach parameters. A hybrid optimisation algorithm associating a genetic algorithm with a Levenberg-Marquardt method [21] is applied for identifying the model parameters. A single set of parameters for all orientation curves is retrieved: $\eta = 1.61$, $\gamma = 2.084$, $\kappa = 0.037$, $\omega = 2.962$ and $\alpha = 0.317$.
The new approach is compared to the FE model in Fig. 6.

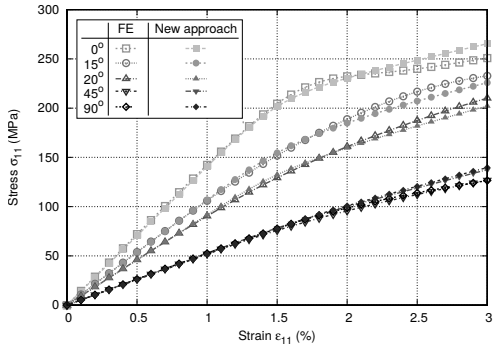

Figure 6: Comparison of strain-stress curves between FE model with cohesive elements and the present model for various loading directions for the PA66-GF30 composite.

Strain-stress curves at 45^o and 90^o are close which confirms this well known result. With the FE tensile test at 0^o, an inflection point is captured. The new approach is able to capture the debonding considered FE model. Debonding initiations and the asymptotic behavior for each orientation are well reproduced while a single set of parameter is used with the new approach. The only weak point is the miss of the

Excerpt from ISBN 978-3-00-053387-7

inflection point captured at 0^o in the new approach.

6. Conclusion

Based on the experimental observations, a strategy to model interfacial damage of short fiber reinforced composites has been build. A probabilistic damage evolution law based on a rupture criterion has been proposed. The quadratic criterion depends on the normal and tangential local stress components at the fiber-matrix interface. It determines a probability of rupture accounted for computing the evolution of the damage ratio. The interfacial damage law is then estimated on the entire ellipsoid surface by varying the angular step. Using this latter and the SLM model, the global load transfer from the matrix to the fiber is determined.

A comparison with a numerical reference solution based on the FE analysis with cohesive elements at the matrix-inclusion interfaces was performed to model a PA66-GF30 composite. It demonstrates the capabilities of the approach to simulate the behavior of short-fiber composites under various loading directions. To model the composite with the new damage model, a two phase incremental Mori-Tanaka scheme is formulated accounting for the proposed stress transfer law. Using a single set of parameters, a good correlation is achieved between FE model and the new approach for all orientations.

Adopting small steps yields to time consuming simulations but the computations still remain faster (roughly 100 times) than those based on the cohesive FE analyses. For structure simulations using the developed approach, an optimized procedure is required to identify the critical damage points. This aspect will be considered in a future work.

Acknowledgments

The support of the FUI project Durafip, driven by Dr. Gilles Robert of Solvay Engineering Plastics, is warmly acknowledged.

References

[1] M.F. Arif, N. Saintier, F. Meraghni, J. Fitoussi, Y. Chemisky, and G. Robert. Multiscale fatigue damage characterization in short glass fiber reinforced polyamide-66. *Composites Part B: Engineering*, 61:55–65, May 2014.

[2] N. Sato, T. Kurauchi, S. Sato, and O. Kamigaito. Microfailure behaviour of randomly dispersed short fibre reinforced thermoplastic composites obtained by direct SEM observation. *Journal of Materials Science*, 26(14):3891–3898, 1991.

[3] F. Meraghni, F. Desrumaux, and M.L. Benzeggagh. Implementation of a constitutive micromechanical model for damage analysis in glass mat reinforced composite structures. *Composites Science and Technology*, 62(16):2087 – 2097, 2002.

[4] R. M. Christensen and K. H. Lo. Solutions for effective shear properties in three phase sphere and cylinder models. *Journal of the Mechanics and Physics of Solids*, 27(4):315–330, August 1979.

[5] Z. Hashin. Thermoelastic properties of fiber composites with imperfect interface. *Mechanics of Materials*, 8(4):333–348, February 1990.

[6] Z. Hashin. Thin interphase/imperfect interface in elasticity with application to coated fiber composites. *Journal of the Mechanics and Physics of Solids*, 50(12):2509–2537, December 2002.

[7] Y. Benveniste and T. Miloh. Imperfect soft and stiff interfaces in two-dimensional elasticity. *Mechanics of Materials*, 33(6):309–323, June 2001.

[8] Z. Zhong and S. A. Meguid. On the Elastic Field of a Shpherical Inhomogeneity with an Imperfectly Bonded Interface. *Journal of Elasticity*, 46(2):91–113, 1997.

[9] H. L. Cox. The elasticity and strength of paper and other fibrous materials. *British Journal of Applied Physics*, 3(3):72, 1952.

[10] A. Jain, Y. Abdin, W. Van Paepegem, I. Verpoest, and S. V. Lomov. Effective anisotropic stiffness of inclusions with debonded interface for eshelby-based models. *Composite Structures*, 131:692 – 706, 2015.

[11] T.W. Clyne and P.J. Withers. *An Introduction to Metal Matrix Composites*. Cambridge University Press, 1993.

[12] J. A. Nairn. On the use of shear-lag methods for analysis of stress transfer in unidirectional composites. *Mechanics of Materials*, 26(2):63–80, September 1997.

[13] M.F. Arif, F. Meraghni, Y. Chemisky, N. Despringre, and G. Robert. In situ damage mechanisms investigation of PA66/GF30 composite: Effect of relative humidity. *Composites Part B: Engineering*, 58:487–495, March 2014.

[14] L. N. McCartney. Stress transfer mechanics for multiple perfectly bonded concentric cylinder models of unidirectional composites. *NPL Report DMM(A)*, 129, 1993.

[15] S. Li and A. Wongsto. Unit cells for micromechanical analyses of particle-reinforced composites. *Mechanics of Materials*, 36(7):543–572, July 2004.

[16] D. W. Spring and G. H. Paulino. A growing library of three-dimensional cohesive elements for use in ABAQUS. *Engineering Fracture Mechanics*, 126:190–216, August 2014.

[17] K. Park, G. H. Paulino, and J. Roesler. Cohesive fracture model for functionally graded fiber reinforced concrete. *Cement and Concrete Research*, 40(6):956–965, 2010.

[18] C. Starke, W. Beckert, and L. B. Lauke. Charakterisierung des delaminationsverhaltens von schichtverbunden unter mode i und mode iibelastungen. *Materialwissenschaft und Werkstofftechnik*, 27:080–089, February 1996.

[19] D.C. Lagoudas, A.C. Gavazzi, and H. Nigam. Elastoplastic behavior of metal matrix composites based on incremental plasticity and the mori-tanaka averaging scheme. *Computational Mechanics*, 8(3):193–203, 1991.

[20] F. Meraghni, C.J. Blakeman, and M.L. Benzeggagh. Effect of interfacial decohesion on stiffness reduction in a random discontinuous-fibre composite containing matrix microcracks. *Composites Science and Technology*, 56(5):541–555, January 1996.

[21] Y. Chemisky, F. Meraghni, Bourgeoisn N., S. Cornell, R. Echchorfi, and E. Patoor. Analysis of the deformation paths and thermomechanical parameter identification of a shape memory alloy using digital image correlation over heterogeneous tests. *International Journal of Mechanical Sciences*, 9697:13 – 24, 2015.

Excerpt from ISBN 978-3-00-053387-7